

Thermoelectric performances of two-dimensional electronic heat engine and refrigerator

Xiaoguang Luo^{*}, Kailin Long, Jun Wang, and Teng Qiu^{*}
Department of Physics, Southeast University, Nanjing 211189, China

Jizhou He
Department of Physics, Nanchang University, Nanchang 330031, China

Abstract

Based on the electronic transport theory, two-dimensional thermoelectric devices (including heat engines and refrigerators) with three different kinds of momentum filters (k_x -, k_y -, and k_z -filters) are established respectively. Following the Fermi-Dirac distribution of electrons, the expressions of some important performance parameters are derived step-by-step for the resonant transport, in which the transmission of electrons is approximated by Lorentzian function. Several optimizations are carried out and the corresponding optimized parameters are found, such as the universal upper bound of efficiency at maximum power of heat engines, maximum coefficient of performance of refrigerators *etc.* From the results, it is found that k_z -filter is the best for thermoelectric performances. After focus on the refrigerators for three filtered cases, an optimum range $< 2k_B T$ of the full width at half maximum of the transport resonance is found for better thermoelectric performances.

PACS number(s): 05.70.Ln, 05.30.Fk, 84.60.Rb, 73.63.-b

I. Introduction

Recent years, thermoelectric materials have attracted great interest due to the endless energy conversion from useless heat sources [1]. Facing the heat waste and energy crisis in our world, thermoelectric mechanism may pave the way to alleviate the energy challenge. Through thermoelectric Seebeck and Paltier effects, the energy conversion between thermal and electric can be processed forward and backward respectively. The friendly working environment without moving parts make them green and stable, and being very possible to be fabricated by solid state materials. To evaluate a thermoelectric material, the dimensionless thermoelectric figure of merit $ZT = S^2 \sigma T / (k_e + k_l)$ is usually adopted, where S is the Seebeck coefficient (also called as thermal power), σ is the electric conductivity, T is the average temperature of the material with hot/cold junctions (T_{HC}), and k_{el} are thermal conductivity due to electron/lattice. The figure of merit is closely related to the conversion efficiency which is increased by making ZT as large as possible. Generally, bulk materials suffer from a very low figure of merit. The ZT of bulk materials around 1 (corresponding conversion efficiency $< 10\%$) cannot meet the requirements for commercial applications [2]. Therefore, how to enhance ZT is a hot topic in

^{*} Email address: 276718626@qq.com (X. Luo); tqiu@seu.edu.cn (T. Qiu).

this field. With the development of nanotechnology, it is found that making the thermoelectric materials small might break the bottleneck for higher ZT , e.g., $\text{Bi}_2\text{Te}_3/\text{Sb}_2\text{Te}_3$ superlattice [3], silicon nanowires [4], PbSeTe-based quantum dots [5], other complex nanoscaled materials [6] etc. Even right now, ZT is still hard to surpass 3 although larger and larger value is reported in different structured materials. So finding a thermoelectric material with higher ZT is a challenge. From the expression directly, the ways to increase ZT are: (1) increasing the Seebeck coefficient; (2) increasing electric conductivity; (3) reducing thermal conductivity. Few years ago, Hick et al. [7] proposed that the reduced dimensionality of superlattices could be used to enhance the electronic density of states and to obtain high efficiency. Besides, the heat loss due to phonons in low dimensional nanostructured materials can be effectively reduced once the length scale is comparable to the phonon mean-free path. In fact, low dimensional nanostructures with a delta-shaped transport distribution are expected as the best thermoelectric materials [8], especially for the semiconductors [9]. Theoretically, this thermoelectric system can tend to be reversible and the corresponding energy conversion efficiency can achieve the maximum Carnot limit (with efficiency $\eta_c = 1 - \tau$ for power generation and **coefficient of performance (COP)** $\varepsilon_c = \tau / (1 - \tau)$ for cooling, where $\tau = T_c / T_h$), where the figure of merit $ZT \rightarrow \infty$ [10].

It should be noted that bigger does not always mean better for conversion efficiency. Taking the heat engine as an example, the power output tends to zero when the efficiency achieves the Carnot limit. Hence there are some optimizations for meaningful designs, and the most common handling is to find the **efficiency at maximum power (EMP)** and corresponding working conditions. Historically, the most famous EMP limit is the **Curzon-Ahlforn (CA)** efficiency $\eta_{CA} = 1 - \sqrt{\tau}$, which is obtained in an endoreversible Carnot heat engine by using finite-time thermodynamic theory [11]. Actually, CA efficiency is just the upper bound of EMP for low symmetric dissipation Carnot engines [12], not the limit for others. Taking the different statistics of working substance as instances, both Maxwell-Boltzmann [13] and Fermi-Dirac [14] statistics result in a bigger EMP than η_{CA} , and one can also predict that the maximum EMP for Bose-Einstein substance is also bigger than η_{CA} . A region of $\eta_c / 2 < \eta_{\max P} < \eta_c / (2 - \eta_c)$ can be used to bound these EMP limits although also being obtained from low-dissipation Carnot engines [15,16]. Back to the thermoelectric heat engine, the maximum EMP should be bounded by this region.

Most considered theoretical models of thermoelectric devices consist of low-dimensional reservoirs with low-dimensional electronic conductors. For example, the quantum dot between two **one-dimensional (1D)** reservoirs (i.e. 1D-0D-1D system) can enhance the thermoelectric performance effectively through resonant tunneling or energy level hopping [17-20]. And this is still due to the delta-shaped transport distribution of the electronic conductor. Actually, the best thermoelectric can be optimized from the transmission function [21] determined by the conductors. Therefore, multi-dimensional reservoirs with low-dimensional conductors can also exhibit high conversion efficiencies (or ZT), where the low-dimensional conductors can be conceptualized as momentum (or energy) filter [22,23]. In these previous works, the transmission of electrons was idealized and electrons in the free direction were handled by Maxwell-Boltzmann statistics, where the average energy component of electrons in one free direction is just $k_B T / 2$ with the

Boltzmann constant k_B . However, these treatments are not reasonable and the energy component is still very dependent on the Fermi-Dirac distribution of electrons. Therefore, the standard expressions of scattering matrix theory towards the low-dimensional systems (e.g. Landauer-Buttiker formula) should be renormalized for multi-dimensional ones. For no overlap, the model with **two-dimensional (2D)** reservoirs and low-dimensional conductors is chosen to extend the discussion.

Many 2D materials (such as graphene, MoS₂, topological insulator etc.) have become new stars in material science and physics. The thermoelectric effect in these 2D materials seems attractive [24-26] and further study is worthwhile. In this paper, we choose classical 2D electron systems as reservoirs, e.g., those confined in the well of GaAs/AlGaAs interface, and Lorentzian resonant transport as filtered mechanism. We would like to work on the reasonable expressions of thermoelectric parameters for multi-dimensional systems. In the following, in Sec. II, the transport behavior of 2D free electrons is analyzed; in Sec. III, some expressions of thermoelectric performances with different momentum filters are derived; in Sec. IV, several important performance parameters are discussed and optimized in detail. Finally, we summarize some obtained results.

II. Modeling details

For one 2D electronic system, the density of states of electrons can be obtained from

$$dn_{2D} = dn_x dn_y = \frac{1}{h^2} dp_x dp_y dx dy \quad (1)$$

Noting that, not all the electrons in the reservoir are able to leave out, the x component of their momentum should point out first, e.g., $p_x > 0$. In the reservoir with temperature T and chemical potential μ , the electrons are described by Fermi-Dirac distribution function

$f = 1 / \{1 + \exp[(E - \mu) / k_B T]\}$. Considering the edge width L and time interval dt , the volume

will be focused on $\iint dx dy = Lv_x dt$, then the number of the electrons out of the reservoir can be calculated by

$$N = \int_{-\infty}^{\infty} \int_0^{\infty} \frac{2Lv_x dt}{h^2} f dp_x dp_y \quad (2)$$

where the factor of 2 accounts for the degeneracy of electron spin, $p_{x/y} = \hbar k_{x/y}$, $E = (\hbar k)^2 / 2m^*$,

$v_x = \hbar k_x / m^*$ is the group velocity of electrons in x -direction, and m^* is the effective mass of electrons in the reservoir. In this section, m^* is regarded as the mass of free electrons in vacuum m for 2D free electrons for convenience. Therefore the electronic flux flowing out of a reservoir, per unit edge width per unit time, can be expressed as

$$\dot{N} = \int_{-\infty}^{\infty} \int_0^{\infty} \frac{2v_x}{h^2} f dp_x dp_y = \frac{4\sqrt{2m}}{h^2} \int_0^{\infty} \sqrt{E} \cdot f dE \quad (3)$$

After further calculation, the expression of electronic flux can be rewritten as

$$\dot{N} = -\frac{2\sqrt{2\pi m}}{h^2} (k_B T)^{3/2} \text{Li}_{3/2}[-\exp(\mu / k_B T)] , \quad \text{where } \text{Li}_n(x) = \sum_{i=1}^{\infty} \frac{x^i}{i^n} \text{ is polylogarithm}$$

function. This flux will be strengthened with the increasing chemical potential and the increasing temperature, which also indicates that more electrons leave out of the reservoir. It is known that a reservoir will release an amount of heat $E - \mu$ when an electron with energy E leaves. So, the heat flux flowing out of a reservoir is

$$\dot{Q} = \frac{4\sqrt{2m}}{h^2} \int_0^\infty (E - \mu) \sqrt{E} \cdot f dE = \frac{\sqrt{2\pi m}}{h^2} (k_B T)^{3/2} \left[2\mu \text{Li}_{3/2}(-e^{\mu/k_B T}) - 3k_B T \text{Li}_{5/2}(-e^{\mu/k_B T}) \right]. \quad (4)$$

It means that the heat flux is very dependent on the temperature and chemical potential. For the special case of $\mu = 0$, the obtained heat flux can be regarded as the maximum heat flux in some way without parasitic backflow from electrons with energy $E < \mu$, and it reads

$$\dot{Q}_{\max} = \alpha T^{5/2} \quad (5)$$

where $\alpha = \left(3 - \frac{3\sqrt{2}}{4}\right) \frac{\sqrt{2\pi m}}{h^2} k_B^{5/2} \zeta(5/2) \approx 10^{-5} \text{ WK}^{-5/2}$ and $\zeta(5/2) = \text{Li}_{5/2}(1) = 1.34149$ is the

so-called Riemann zeta function. Subsequently, the thermal capacity of the 2D system is

$C_{2D} = \frac{5}{2} \alpha T^{3/2}$ which corresponds to that of $C_{1D} = \frac{\pi^2 k_B^2}{3h} T$ in 1D system [27]. By the way, when

the 1D and 2D reservoirs are regarded as $\frac{1}{2}$ - and $\frac{3}{2}$ -dimensional bathes (half-free in x -direction)

respectively, these relationships between heat flux and temperature seem like the result of the quantum absorption refrigerator $\dot{Q} \propto T^{d+1}$ for d -dimensional bath when $T \rightarrow 0$ [28].

The other usually considered case is that of $\mu > 0$. For the given temperature, Eq. (4) can be simplified by $\dot{Q} = \frac{\sqrt{2\pi m}}{h^2} (k_B T)^{5/2} g(x)$ where $g(x) = 2x \text{Li}_{3/2}(-e^{-x}) - 3 \text{Li}_{5/2}(-e^{-x})$ and $x = \mu / k_B T$. Thus one can easily find maximum heat flux as

$$\dot{Q}_{\max} = \beta T^{5/2} \quad (6)$$

through $\partial \dot{Q} / \partial x = 0$, where $g(x) = 2.91927$ when $x = x_0 = 0.723303$, and $\beta \approx 1.13 \times 10^{-5}$

$\text{WK}^{-5/2}$. In addition, $x = x_0$ implies that a linear relationship exists between the chemical potential and temperature at maximum heat flux, i.e., $\mu = x_0 k_B T \approx 10^{-23} T$. Compared to the case of $\mu = 0$,

the increasing chemical potential of the reservoir is beneficial for higher maximum heat flux (i.e., $\beta > \alpha$), though with the increased parasitic backflow from electrons. As shown in Fig. 1, the difference between the maximum heat flux for $\mu = 0$ and $\mu > 0$ respectively is very remarkable at higher temperature. For example, when $T = 300 \text{ K}$, the maximum heat flux of $\mu = 0$ is 15.6 W, which will reach 17.6 W when $\mu = 0.0187 \text{ eV}$.

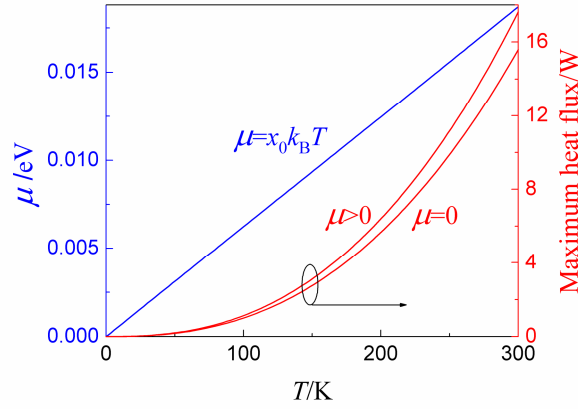


Fig. 1. The situations of maximum heat flux for one reservoir at different temperature. (Right axis) the maximum heat flux when $\mu = 0$ and $\mu > 0$; (left axis) the linear relationship between chemical potential and temperature at maximum heat flux when $\mu > 0$.

To form thermoelectric devices for applications, the simplest and most effective fabrication consists of two electronic reservoirs (or leads) and an electronic conductor between them [10]. Electrons in these reservoirs can also be regarded as free electrons at effective mass assumption, where m in the above equations should be replaced by material-dependent effective mass m^* . As to reservoirs, the cold one should possess the higher chemical potential so that the electrons can be exchanged due to the temperature and chemical potential gradients, that is $T_H > T_C$ and $\mu_C > \mu_H$. The exchanging behavior can also be explained by that, the electrons are often transmitted from the occupied states to the empty states, see the difference between Fermi-Dirac distribution functions of two reservoirs in the inset of Fig. 2a. Heat coupled with the electronic flux from the hot to cold reservoir (against the chemical potential gradient) can be turned into electrical power and the thermoelectric device then performs as a heat engine; on the other hand, the heat in the cold reservoir can be pumped out and flow into the hot reservoir with the help of electrical power input and then the thermoelectric device performs as a refrigerator.

In thermoelectric devices, not all the electrons described by Eq. (2) are available any more for the exchanging system. Many factors such as the Fermi-Dirac distribution, the transmission in the electronic conductor, or even the geometry of the reservoir interfaces [29] *etc.*, might impact the electron exchanging dramatically. Therefore, the number of electrons flowing out of a reservoir per unit time can be expressed as

$$\dot{N}_{H/C} = \frac{2}{h^2} \iint L_{H/C} v_x f_{H/C} (1 - f_{C/H}) t(E_i) dp_x dp_y \quad (7)$$

where integral conditions and the transmission probability $t(E_i)$ are dependent on the reservoir interfaces and the electronic conductors, of which the latter can filter electrons selectively upon their momentums (or energies) and can be tuned by the electrical gating. Ignoring other edge effects, two cases will be considered in the following studies, including frameworks of parallel interfaces of reservoirs with infinite dimension in longitudinal direction and one reservoir encircling the other one concentrically. Due to the quantum confinement or barrier blockage, as illustrated in Fig. 2a-c, there are at least three kinds of filtered mechanism in the 2D thermoelectric

devices, including k_x -, k_y -, and k_r -filters, where $k_r^2 = k_x^2 + k_y^2$. All three kinds of filters can be realized in the parallel case, while in the encircled case k_r -filter is most possible.

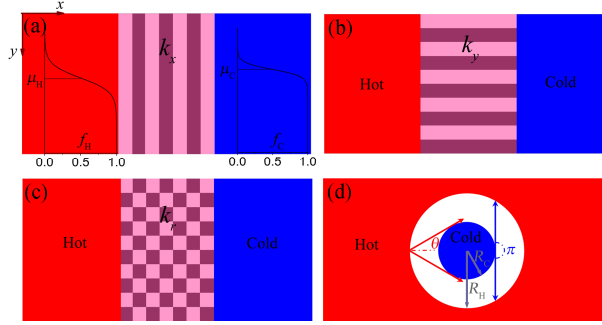


Fig. 2. (a-c) Schematics of three kinds of filtered thermoelectric devices with k_x -, k_y -, and k_r -filters, the insets of (a) are the corresponding Fermi-Dirac distributions of the hot and cold reservoirs, where $\mu_H < \mu_C$. (d) Schematic of the encircled case with cold inner part (R_C) and hot outer part (R_H), where θ is half scattering angle of effective electrons in hot reservoir and the scattering angle of effective electrons in cold reservoir is π .

III. Heat flux of the thermoelectric devices with different filters

For the parallel case with $L_H = L_C$, all the parameters can be obtained per unit length per unit time with no need to consider the whole width. According to Eq. (7), the net electronic flux flowing from hot to cold reservoir can be expressed as $\dot{N} = \dot{N}_H - \dot{N}_C$. Coupled with the particle flux, an amount of heat $E - \mu_{H/C}$ will be released or absorbed by the reservoir when an electron leaves or arrives at hot/cold reservoir. So it is obtained that, per unit length per unit time, the current, heat flux out of the hot/cold reservoir are

$$I = \frac{2e}{h^2} \int_{-\infty}^{\infty} \int_0^{\infty} v_x (f_H - f_C) t(E_i) dp_x dp_y \quad (8)$$

$$\dot{Q}_{H/C} = \frac{2}{h^2} \int_{-\infty}^{\infty} \int_0^{\infty} (E - \mu_{H/C}) v_x (f_{H/C} - f_{C/H}) t(E_i) dp_x dp_y \quad (9)$$

Noting that these two equations are valid for all of k_x -, k_y -, and k_r -filtered parallel cases. On the other hand, we here consider the resonant transport with one resonant peak of the first band, and the transmission probability can be approximated well by a Lorentzian function [30]

$$t(E_i) = \frac{(\Gamma_i / 2)^2}{(E_i - E_i^p)^2 + (\Gamma_i / 2)^2} \quad (10)$$

where $i = x, y, r$ for different filters and $E_r = E$, Γ_i and E_i^p are the **full width at half maximum (FWHM)** and energy center of the resonance respectively.

When this thermoelectric device works as a heat engine, the power output and the efficiency are $P = \dot{Q}_H + \dot{Q}_C$ and $\eta = P / \dot{Q}_H$ respectively. Similarly, once the heat flux flows out of the cold reservoir, the device can perform as a refrigerator, and the cooling rate and COP are $R = \dot{Q}_C$ and

$\varepsilon = R/(-P)$, respectively.

As to the entropy production rate of the system, several ways can be adopted to obtain the same result. When the direction of net electronic flux is from hot to cold reservoir, the entropy increases the amount of $-(E-\mu_H)/T_H+(E-\mu_C)/T_C$ due to each exchanged electron with energy E [10]. So the total entropy production rate of the system is expressed as

$$S = \frac{2}{h^2} \int_{-\infty}^{\infty} \int_0^{\infty} \left(-\frac{E-\mu_H}{T_H} + \frac{E-\mu_C}{T_C} \right) v_x (f_H - f_C) t(E_i) dp_x dp_y, \quad (11)$$

Similarly, when the direction of net electronic flux is from cold to hot reservoir, the entropy increases the amount of $(E-\mu_H)/T_H-(E-\mu_C)/T_C$ due to each electron, and the expression of the total entropy production rate is the same as Eq. (11). Of course, the general derivation from $S = -\dot{Q}_H/T_H - \dot{Q}_C/T_C$ can also recover this expression. Anyway, it should be noted that this expression is also valid for k_x -, k_y -, and k_r -filtered cases, and from which one can find that $S \geq 0$.

A. k_r -filter

The encircled case is easily studied for k_r -filter. The length of the reservoir interface is $L_{\text{H/C}} = 2\pi R_{\text{H/C}}$. If fixing the inner part as the cold reservoir, as shown in Fig. 2d, all electrons out of the cold reservoir are possible to arrive at the hot one, but it is not for the electrons out of the hot reservoir. Only the electrons locating in the scattering angle 2θ are effective for the thermoelectric effect, where $\sin\theta = R_C/R_H$. In this case, Eq. (7) can be rewritten by the following two equations

$$\dot{N}_H^r = \frac{2L_H}{m^*h^2} \int_0^{\infty} \int_{-\theta}^{\theta} p_r^2 \cos\theta' f_H (1-f_C) d\theta' dp_r = \frac{4\sqrt{2m^*}L_C}{h^2} \int_0^{\infty} \sqrt{E} f_H (1-f_C) t(E) dE \quad (12a)$$

$$\dot{N}_C^r = \frac{2L_C}{m^*h^2} \int_0^{\infty} \int_{-\pi/2}^{\pi/2} p_r^2 \cos\theta' f_C (1-f_H) d\theta' dp_r = \frac{4\sqrt{2m^*}L_C}{h^2} \int_0^{\infty} \sqrt{E} f_C (1-f_H) t(E) dE \quad (12b)$$

These interesting results imply that the electronic flux out of the outer part is very dependent on the interface length of the inner part, but not both parts. Therefore, Eqs. (8) and (9) are still valid for the encircled case with k_r -filter per unit length of the inner reservoir interface. The heat flux flowing out of the reservoirs with k_r -filter considered in this paper can be represented as

$$\dot{Q}_{\text{H/C}}^r = \int_0^{\infty} \Psi_{\text{H/C}}^r(E) t(E) dE \quad (13a)$$

$$\Psi_{\text{H/C}}^r(E) = \frac{4\sqrt{2m^*}}{h^2} (E - \mu_{\text{H/C}}) \sqrt{E} (f_{\text{H/C}} - f_{\text{C/H}}) \quad (13b)$$

B. k_x -filter and k_y -filter

The total energy of an electron can be rewritten as $E = E_x + E_y$, and the corresponding 2D Schrödinger's equation can be separated into transverse and longitudinal parts. Therefore, some

structures (such as quantum well) can filter electrons based on the momentum (or energy) component in one direction, as shown in Fig. 2a and 2b. During the exchanging, the electrons are confined in the filtered direction but considered to be free in the other one direction. In that case, O'Dwyer et al. [23] assumed that electrons in the free direction follow Maxwell-Boltzmann statistics, with which the average energy component for each degree of freedom can be easily calculated as $k_B T / 2$. However, it is not reasonable. Here we do all calculations directly from the original equations with Fermi-Dirac statistics.

For the parallel case with k_x -filter, the electronic flux out of the reservoir can be calculated by Eq. (9). The final expressions can also be in the form of Eq. (13) when the energy E and function $\Psi_{\text{H/C}}^r(E)$ is replaced by energy component E_x and $\Psi_{\text{H/C}}^x(E_x)$ respectively, where

$$\Psi_{\text{H/C}}^x(E_x) = \frac{\sqrt{2\pi m}}{h^2} \left\{ \begin{aligned} & 2(E_x - \mu_{\text{H/C}}) \left\{ \sqrt{k_B T_{\text{CH}}} \text{Li}_{1/2} \left[-e^{-(E_x - \mu_{\text{CH}})/k_B T_{\text{CH}}} \right] - \sqrt{k_B T_{\text{HC}}} \text{Li}_{1/2} \left[-e^{-(E_x - \mu_{\text{HC}})/k_B T_{\text{HC}}} \right] \right\} \\ & + (k_B T_{\text{CH}})^{3/2} \text{Li}_{3/2} \left[-e^{-(E_x - \mu_{\text{CH}})/k_B T_{\text{CH}}} \right] - (k_B T_{\text{HC}})^{3/2} \text{Li}_{3/2} \left[-e^{-(E_x - \mu_{\text{HC}})/k_B T_{\text{HC}}} \right] \end{aligned} \right\} \quad (14)$$

Similarly, k_y -filter can be realized in the other parallel case, see Fig. 2b. The electrons in the electronic conductor are confined in y -direction and half-free in x -direction (e.g., $k_x > 0$). Therefore, from Eq. (9), the expressions of heat flux flowing out of the reservoirs also have the form of Eq. (13) when the energy E and function $\Psi_{\text{H/C}}^r(E)$ is replaced by energy component E_y and $\Psi_{\text{H/C}}^y(E_y)$ respectively, and

$$\Psi_{\text{H/C}}^y(E_y) = \frac{2\sqrt{2m/E_y}}{h^2} \left\{ \begin{aligned} & (E_y - \mu_{\text{H/C}}) \left\{ k_B T_{\text{HC}} \log \left[1 + e^{-(E_y - \mu_{\text{HC}})/k_B T_{\text{HC}}} \right] - k_B T_{\text{CH}} \log \left[1 + e^{-(E_y - \mu_{\text{CH}})/k_B T_{\text{CH}}} \right] \right\} \\ & - (k_B T_{\text{HC}})^2 \text{Li}_2 \left[-e^{-(E_y - \mu_{\text{HC}})/k_B T_{\text{HC}}} \right] + (k_B T_{\text{CH}})^2 \text{Li}_2 \left[-e^{-(E_y - \mu_{\text{CH}})/k_B T_{\text{CH}}} \right] \end{aligned} \right\}. \quad (15)$$

IV. Performances and optimum analysis of thermoelectric heat engines and refrigerators with different filters

A. $\Gamma_i \rightarrow \infty$

It is noted that the case without filtering is a trivial situation of k_r -filter, i.e., $\Gamma_r \rightarrow \infty$ and $t(E) = 1$ for all transmitted electrons. And actually, the three filtered cases are equivalent to each other when $\Gamma_{x/y} \rightarrow \infty$. Even so, the thermoelectric devices at these conditions can still work as heat engines or refrigerators in theory. One can confirm it by the positive power output or positive cooling rate. From Eq (9), the possible relative power output and relative cooling rate of the device can be calculated as

$$P^* = P / \frac{\sqrt{2\pi m^*}}{h^2} (k_B T_{\text{H}})^{5/2} = 2(x_{\text{H}} - \tau x_{\text{C}}) \left[\text{Li}_{3/2}(-e^{x_{\text{H}}}) - \tau^{3/2} \text{Li}_{3/2}(-e^{x_{\text{C}}}) \right] \quad (16a)$$

$$R^* = \dot{Q}_{\text{C}} / \frac{\sqrt{2\pi m^*}}{h^2} (k_B T_{\text{H}})^{5/2} = 2\tau^{5/2} x_{\text{C}} \text{Li}_{3/2}(-e^{x_{\text{C}}}) - 3\tau^{5/2} \text{Li}_{5/2}(-e^{x_{\text{C}}}) - 2\tau x_{\text{C}} \text{Li}_{3/2}(-e^{x_{\text{H}}}) + 3\text{Li}_{5/2}(-e^{x_{\text{H}}})$$

(16b)

where the dimensionless scaled chemical potential $x_{H/C} = \mu_{H/C} / k_B T_{H/C}$. Thus, at a given hot reservoir temperature T_H , the working region of this thermoelectric device can be determined by $P^* > 0$ and $R^* > 0$. From numerical calculations, also see partly in Fig. 3, the working region of heat engine extends firstly and then shrinks gradually. When $\tau \rightarrow 1$, both boundaries of the working region tend to the line of $x_H = x_C$ and the region vanishes. However, the thermoelectric device works as a refrigerator only when $\tau > 0.691226$. The cooling region with respect to $x_{H/C}$ looks like a part twisted leaf shape, and it will be stretched when τ increases. And when $\tau \rightarrow 1$, the maximum x_H of the cooling region tends to infinity and the boundary close to the heat engine working region tend to the line of $x_H = x_C$ from above.

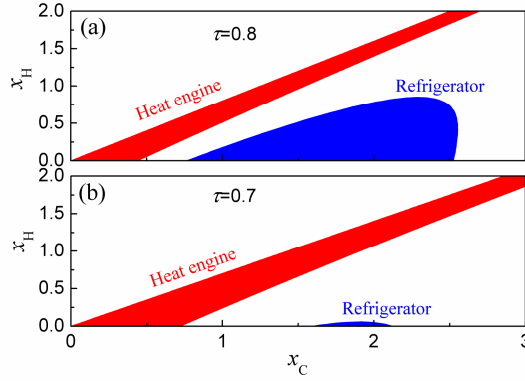


Fig. 3. The working region of heat engine and refrigerator at $\tau = 0.7$ and $\tau = 0.8$ when $\Gamma_i \rightarrow \infty$.

These trivial working conditions are only in the ideal hypothesis, and cannot achieve optimal performances. Generally, the energy spectrum of the electrons in the thermoelectric device can be divided into three regions by the energy positions of μ_C and $E_0 = (\mu_C T_H - \mu_H T_C) / (T_H - T_C)$ [10,23]. When the energies of exchanged electrons locate in $\mu_C < E < E_0$, the corresponding net electronic flux will flow from cold to hot reservoir because of $f_C > f_H$. And according to Eq. (9), the heat flux will follow the same direction, as a result, the thermoelectric device works as a refrigerator. Similarly, if the energies of transmitted electrons locate in $E > E_0$, the thermoelectric device works as a heat engine because of the net electronic flux flows against the chemical potential gradient (from hot to cold reservoir). Therefore, filtering the electrons in the exchanging process will be more practical and available.

B. $\Gamma_i \ll k_B T$

To filter electrons as needed, the structures of quantum dots or quantum wells are often used. In these nanostructures, the case of transmission spectra with one resonance is a simple and effective filter when the subbands are far away from the chemical potentials, around which by several $k_B T$ the electron-exchanging happens. As the FWHM of the resonance decreases to a very small value, there only few electrons are transmitted by the electronic conductor due to the Coulomb-block, which is an effective way to improve the efficiencies of the thermoelectric devices [10,14]. Here the limit of $\Gamma_i \ll k_B T$ will be discussed for this kind of filters. After several algebraic steps, the heat fluxes out of the reservoirs (Eq. (9)) and the total entropy

production rate of the system (Eq. (11)) can be analytically approximated as

$$\dot{Q}_{\text{H/C}}^i = \frac{\pi\Gamma_i}{2} \Psi_{\text{H/C}}^i(E_i^{\text{p}}) \quad (17)$$

and

$$S^i = -\frac{\pi\Gamma_i}{2} \left[\frac{\Psi_{\text{H}}^i(E_i^{\text{p}})}{T_{\text{H}}} + \frac{\Psi_{\text{C}}^i(E_i^{\text{p}})}{T_{\text{C}}} \right] \quad (18)$$

respectively, where $i = r, x, y$. The heat fluxes are very weak because of the small FWHM, while the efficiencies of the thermoelectric devices in this case are sufficient. Similar to 1D-0D-1D and 3D-0D-3D systems, the efficiency/COP of the k_r -filtered case are expected as $\eta^r = \frac{\mu_{\text{C}} - \mu_{\text{H}}}{E_r^{\text{p}} - \mu_{\text{H}}}$ for

a heat engine and $\varepsilon^r = \frac{E_r^{\text{p}} - \mu_{\text{C}}}{\mu_{\text{C}} - \mu_{\text{H}}}$ for a refrigerator. They are the maximum values for varied

FWHMs under given chemical potentials [10,23]. Besides, they both tend to Carnot values once $E_r^{\text{p}} \rightarrow E_0$, as shown in Fig. 4, which are independent on the temperatures directly. Meanwhile, the

entropy production rate vanishes and the system becomes reversible. The same situation does not happen in $k_{x/y}$ -filtered case. Owing to the degree of freedom, the entropies in $k_{x/y}$ -systems are

always increased until the exchanging being cutoff at high energy. As to efficiencies or COPs at the given parameters, see Fig. 4a, higher maximum-values can often be obtained by k_x -filtered systems but not k_y -filtered ones.

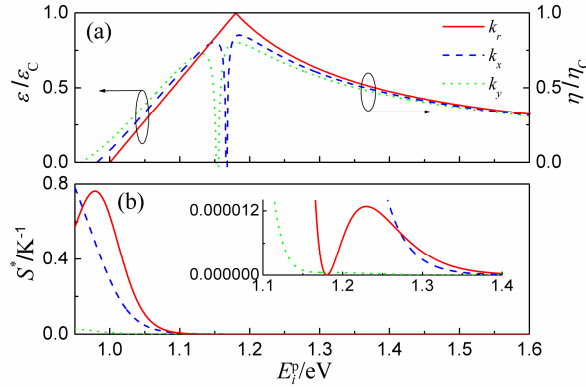


Fig. 4. Performance properties of thermoelectric devices when $\Gamma_i \ll k_{\text{B}}T$. (a) Relative COPs (right axis) and relative efficiencies (left axis) of thermoelectric devices working as refrigerator and heat engine respectively. (b) The relative entropy production rate of the system $S^* = S/\Gamma$ (SI), inset is partial enlarged detail. The parameters are given as $\mu_{\text{C}} = 1\text{eV}$, $\mu_{\text{H}} = 0.98\text{eV}$, $T_{\text{C}} = 270\text{K}$, $T_{\text{H}} = 300\text{K}$ and $m^* = 0.067m$ for GaAs,

Table 1. Different thermoelectric contributions of the electrons in different energy regions, parameters are the same as those in Fig. 4.

Filters	Refrigerator (eV)	Heat engine (eV)
k_r	$1 < E < 1.18$	$E > 1.18$
k_x	$0.98113 < E_x < 1.16605$	$E_x > 1.16774$
k_y	$0.957653 < E_y < 1.15207$	$E_y > 1.15548$

Table 1 shows some interesting results from the data of Fig. 4a. For k_r -filtered case, thermoelectric device works as a refrigerator for the electrons with energy in the region of $\mu_C < E < E_0$ and works as a heat engine for $E > E_0$. The remaining electrons in the trivial region of $E < \mu_C$ contribute nothing but help to heat the cold reservoir. Similar situations happen in the $k_{x/y}$ -filtered case. However, an additional trivial region exists between working regions of the refrigerator and heat engine although it is very small, i.e., $1.16605\text{eV} < E_x < 1.16774\text{eV}$ for k_x -filtered case and $1.15207\text{eV} < E_y < 1.15548\text{eV}$ for k_y -filtered case. This is very different from that of k_r -filtered case, and the abnormal gap should ascribe to the degree of freedom in the other direction. During the exchanging, the heat brought out of cold reservoir by the net electronic flux cannot offset the intrinsic heat leak (due to the temperature gradient) flowing from hot to cold reservoir any more. And it seems that the k_y -filtered case leaks more heat.

Those comparisons with respect to E_i^p (but not the whole energy) make no sense. Instead, the maximum value may be valid for these evaluations. From Eqs. (14), (15) and (17), the efficiencies or COPs of $k_{x/y}$ -filtered cases are very dependent on the temperatures. Taking the heat engines as examples, the upper bound upon the efficiencies can be obtained in the limit that $\kappa = (\mu_C - \mu_H) / k_B (T_H - T_C) \gg 1$, and the maximum efficiencies are obtained when $E_i^p = E_0$ [23]. That may be the reason why the maximum efficiencies appear around E_0 in Fig. 4a. After handling like that, the analytical expressions for $k_{x/y}$ -filtered heat engine are given by

$$\eta^x = \eta_C \left[1 + \eta_C \left(k_B T_C + k_B T_H + k_B \sqrt{T_C T_H} \right) \Lambda(\kappa) / 2eV_0 \right]^{-1} \quad (19a)$$

$$\eta^y = \eta_C \left[1 - \eta_C \left(k_B T_C + k_B T_H \right) \Omega(\kappa) / eV_0 \right]^{-1} \quad (19b)$$

respectively, where $\Lambda(\kappa) = \text{Li}_{3/2}(-e^{-\kappa}) / \text{Li}_{1/2}(-e^{-\kappa})$ and $\Omega(\kappa) = \text{Li}_2(-e^{-\kappa}) / \log(1 + e^{-\kappa})$ tend to 1 and -1 respectively when $\kappa \gg 1$. From these two equations, one can easily find that the upper bound $\eta^x > \eta^y$ at a fixed bias V_0 because of $T_C + T_H > \sqrt{T_C T_H}$, and both of them are smaller than the Carnot value. Therefore, compared to k_y -filter, k_x -filtered case is indeed more suitable for heat engine. This method cannot be adopted to deal with the refrigerators because $\dot{Q}_C^{x/y} < 0$

when $E_{x/y}^p \rightarrow E_0$, but it can be confined that the maximum COP of k_x -filtered refrigerator is larger than that of k_y -filtered one through more numerical simulations, not shown here. So, when the k_r -filter is difficult to be realized, k_x -filter may be an alternative way to obtain higher efficiencies.

In addition to the maximum efficiency, the power output is also a very important parameter for a heat engine. However, it nearly vanishes when the efficiency reaches the maximum value. Similar phenomenon happens in a refrigerator. In order to get the optimized working conditions, a target function of $\chi = \zeta \dot{Q}_{\text{out}}$ is usually used, where ζ indicates the efficiency or COP and \dot{Q}_{out} denotes the heat flux flowing out of the target reservoir, e.g., $\chi = \eta \dot{Q}_{\text{H}}$ for a heat engine and $\chi = \varepsilon \dot{Q}_{\text{C}}$ for a refrigerator [31]. By maximizing this target function, τ -dependent upper bounds can be found, e.g., the CA efficiency $\eta_{\text{CA}} = 1 - \sqrt{\tau}$ and CA COP $\varepsilon_{\text{CA}} = 1 / (1 - \sqrt{1 - \tau}) - 1$ for a low symmetric dissipation Carnot engine and refrigerator respectively [12]. And there are many works upon different models by using these approaches [32-35].

For heat engine, the target function equals to the power output, i.e., $\chi = P$, so that the optimization is turned into finding the EMP, which is a very meaningful parameter in practical applications. Considering the convenience for calculations, the power of those three kind of k_i -filtered heat engines are written from Eqs. (13-15) and (17) as

$$P^r = \frac{2\pi\Gamma_r k_B T_H \sqrt{2m^* E_r^p}}{h^2} [\lambda_{\text{H}}^r - (1 - \eta_{\text{C}}) \lambda_{\text{C}}^r] \left(\frac{1}{1 + e^{\lambda_{\text{H}}^r}} - \frac{1}{1 + e^{\lambda_{\text{C}}^r}} \right) \quad (20a)$$

$$P^x = \frac{\pi\Gamma_x (k_B T_H)^{3/2} \sqrt{2\pi m^*}}{h^2} [\lambda_{\text{H}}^x - (1 - \eta_{\text{C}}) \lambda_{\text{C}}^x] \left[\sqrt{1 - \eta_{\text{C}}} \text{Li}_{1/2}(-e^{-\lambda_{\text{C}}^x}) - \text{Li}_{1/2}(-e^{-\lambda_{\text{H}}^x}) \right] \quad (20b)$$

$$P^y = \frac{\pi\Gamma_y (k_B T_H)^2 \sqrt{2m^* / E_y^p}}{h^2} [\lambda_{\text{H}}^y - (1 - \eta_{\text{C}}) \lambda_{\text{C}}^y] \left[\log(1 + e^{-\lambda_{\text{H}}^y}) - (1 - \eta_{\text{C}}) \log(1 + e^{-\lambda_{\text{C}}^y}) \right] \quad (20c)$$

where $\lambda_{\text{H/C}}^i = (E_i^p - \mu_{\text{H/C}}) / k_B T_{\text{H/C}}$ are dimensionless scaled energies. The optimizations can be produced focusing on the chemical potentials $\mu_{\text{H/C}}$ and temperature ratio τ (or Carnot efficiency $\eta_{\text{C}} = 1 - \tau$), so here T_{H} and E_i^p can be considered as arbitrary constant, and Γ_i can be regarded as a small constant too. After giving T_{H} , E_i^p and Γ_i , the maximum power can be obtained through $\partial P^i / \partial \lambda_{\text{H}}^i = \partial P^i / \partial \lambda_{\text{C}}^i = 0$. And then, the EMPs can be obtained by numerical calculations, as shown in Fig. 5. $\lambda_{\text{C}}^i \geq \lambda_{\text{H}}^i$ can be derived from the total entropy production rate of systems (Eq. (18)) which corresponding the numerical results here.

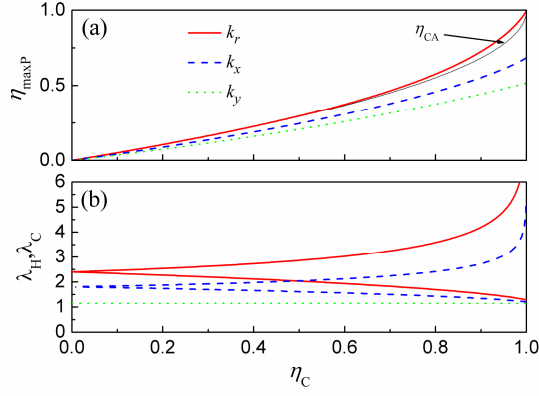


Fig. 5. (a) Efficiencies at maximum power for the k_r -, k_x - and k_y -filtered heat engines, CA efficiency is smaller than k_r -filtered case but much larger than the other two cases. (b) The corresponding dimensionless scaled energies of (a), each pair curves indicate λ_C^i (upper) and λ_H^i (lower) respectively, while $\lambda_C^y = \lambda_H^y = 1.14455$ for k_y -filtered case.

From the results, it is clearly shown that the EMP of k_r -filtered heat engine is larger than those of two others, and the k_y -filtered case is the smallest one. Moreover, the former one is slightly larger than the CA efficiency, while the two latter ones are much less than it. And in fact, the EMP of k_r -filtered heat engine equals to that of 1D-0D-1D system with quantum dot [14], which might be because of the same Fermi-Dirac statistics and total scaled energy. All the EMPs of three cases increase from 0 to a maximum value when Carnot efficiency increases from 0 to 1. However, maximum efficiencies are different from each other, i.e., 1, 0.686552, and 0.516548 respectively. For the k_y -filtered case, $\lambda_C^i = \lambda_H^i$ can be obtained from $\partial P^i / \partial \lambda_H^i = \partial P^i / \partial \lambda_C^i = 0$, and both of them can be calculated as 1.14455 at the maximum power, also shown in Fig. 5b. More interesting, the efficiency at maximum power of this case is $\eta_{\max P}^y = \eta_C / (2.87186 - 0.93593\eta_C)$, which is the same as the result of 1D system when $\Gamma \rightarrow \infty$ [36].

The results here can be explained as that, the energy level in the k_y electronic conductor tends to the single level when Γ_y is small enough, then the 2D system degenerates into 1D one and is equivalent to the 1D system with $\Gamma \rightarrow \infty$ because of the half-freedom in x -direction (e.g., $k_x > 0$).

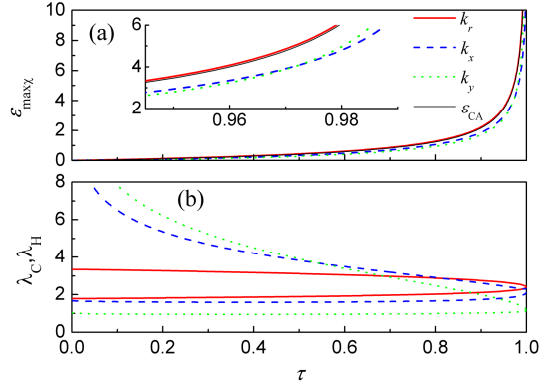


Fig. 6. (a) COPs at maximum χ for the k_r -, k_x - and k_y -filtered refrigerators, the so-called CA COP is a little smaller than k_r -filtered case but larger than the other two cases, the size relation of k_x - and k_y -filtered cases reverses around $\tau = 0.972$. (b) The corresponding dimensionless scaled energies of (a), each pair curves indicate λ_H^i (upper) and λ_C^i (lower) respectively.

Similar results can be found in the refrigerator. From $\partial\chi^i / \partial\lambda_H^i = \partial\chi^i / \partial\lambda_C^i = 0$, the COP at maximum χ (i.e. $\varepsilon_{\max\chi}$ in Fig. 6(a)) can be obtained by numerical calculations. As expected, the $\varepsilon_{\max\chi}^r$ of k_r -filtered refrigerator is a little larger than the CA COP ε_{CA} , which is also larger than those of $k_{x/y}$ -filtered refrigerators. The difference is that dimensionless scaled energies $\lambda_C^i \leq \lambda_H^i$ right now (see Fig. 6(b)), which can also be derived from $S^i \geq 0$. Moreover, $\varepsilon_{\max\chi}^x > \varepsilon_{\max\chi}^y$ when $\tau < 0.972$, and this might be due to the larger enough cooling rate of k_y -filtered refrigerators than that of k_x -filtered refrigerators when $\tau > 0.972$.

C. Γ_i is of several $k_B T$

In addition to the two limiting cases above, there is a more practical situation between them when Γ_i is just few $k_B T$. Without doubt, the performances are bounded by those of two limiting cases above but more close to feasible thermoelectric devices. Many works have done about the optimizations of these performances, especially upon the heat engine. Taking the 1D heat engine with a quantum dot as an example [37], both the maximum efficiency and EMP decrease monotonously when the Γ increases, and of course the maximum efficiency is always larger than the EMP. The maximum power increases firstly and then slides down slowly, while it reaches the peak at about $\Gamma \approx 2.25k_B T$. For the sake of differing from the previous works, we next chose the refrigerator to discuss further.

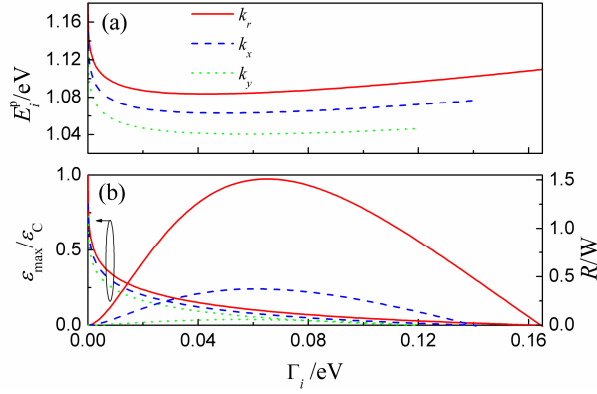


Fig. 7. Maximum COP with respect to FWHM Γ_i for k_r -, k_x - and k_y -filtered refrigerators. (a) The corresponding energy center of the resonance E_i^p . (b) Relative maximum COP (left axis) and the corresponding cooling rate at maximum COP (right axis). Other parameters are given as the same as those in Fig. 4.

Fig. 7 shows the results of maximum COP ε_{\max}^i with respect to Γ_i for the three filtered refrigerator models. It shows clearly that all ε_{\max}^i decrease monotonously with different initial values when the Γ_i increases gradually, i.e. ε_C , $0.807337\varepsilon_C$, and $0.7275\varepsilon_C$ for k_r -, k_x - and k_y -filtered refrigerators respectively (also shown in Fig. 4(a)). The corresponding energy centers of the resonance E_i^p decrease firstly and then regain slightly from the initial values of 1.18, 1.1504, and 1.13095 eV for k_r -, k_x - and k_y -filtered refrigerators respectively. All the cooling rates at maximum COP increase firstly and then slide down until vanishing. This is different from the situation of heat engine because of the finite cooling region. Anyway, k_r -filter is most beneficial to ε_{\max}^i and cooling rate at maximum COP, then the k_x -filter, and then the k_y -filter.

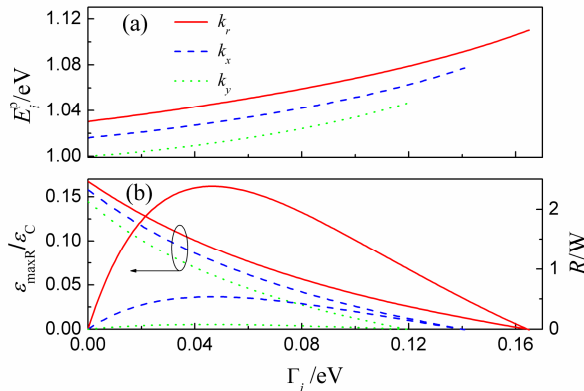


Fig. 8. COP at maximum cooling rate with respect to FWHM Γ_i for k_r -, k_x - and k_y -filtered refrigerators. (a)

The corresponding energy center of the resonance E_i^p . (b) Relative COP at maximum cooling rate (left axis) and the corresponding maximum cooling rate (right axis). Other parameters are given as the same as those in Fig. 4.

Likewise, in addition to the maximum COPs, the COPs at maximum cooling rate $\varepsilon_{\max R}^i$ are very important performance parameters for finite Γ_i and even seem more meaningful in practical applications. Fig. 8 shows the numerical results of $\varepsilon_{\max R}^i$ at the same given parameters as in Fig. 4. When Γ_i increases gradually from 0 to few electron volts, all the maximum cooling rates of three filtered refrigerators increase firstly and finally decrease to 0, and all the $\varepsilon_{\max R}^i$ decrease monotonously. In addition, the corresponding energy centers of the resonance E_i^p increase monotonously. Compared to ε_{\max}^i in Fig. 7, $\varepsilon_{\max R}^i$ are much smaller at the small Γ_i , while they are comparable when Γ_i increases. More interesting, maximum cooling rates of the three cases peak around $\Gamma_i \approx 2k_B T$ (also see Table 2), which corresponds to the result in reference [37] where the power of heat engine with a quantum dot peaks at about $\Gamma \approx 2.25k_B T$.

Generally, the maximum efficiency or maximum COP can be predicted by the thermoelectric figure of merit ZT from [38]

$$\eta_{\max} = \frac{M-1}{M+\tau} \eta_C \quad (21a)$$

$$\varepsilon_{\max} = \frac{M-1/\tau}{M+1} \varepsilon_C \quad (21b)$$

where $M = \sqrt{1+ZT}$. On the contrary, ZT can be estimated from the calculated maximum efficiency or maximum COP. Here we also choose the refrigerators as examples. Based on the data in Fig. 7, ZT decreases monotonously with the increasing FWHM for all of three filtered refrigerators, as depicted in Fig. 9. The maximum values of ZT ($\Gamma_i \rightarrow 0$) are shown in Table 2, i.e., ∞ , 98.1559, and 44.5247 for k_r -, k_x - and k_y -filtered refrigerators respectively. It clearly shows that k_r -filter is most beneficial to the thermoelectric figure of merit, then the k_x -filter, and then the k_y -filter. Narrower FWHM is beneficial for higher ZT but it suppresses the cooling rate. So the better strategy is choosing one value of Γ_i from 0 to $2k_B T$, although ZT is relatively small when $\Gamma_i \approx 2k_B T$ (see Table 2). Finally, it should be noted that the numerical calculations above do not include the heat loss and the COP and ZT are actually overestimated in some degree.

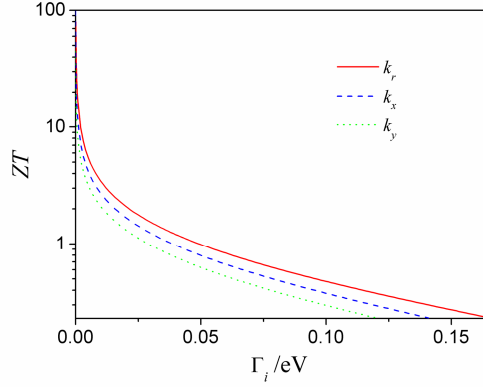


Fig. 9. The estimated thermoelectric figure of merit ZT with respect to FWHM Γ_i for k_r -, k_x - and k_y -filtered refrigerators. Other parameters are given as the same as those in Fig. 4.

Table 2. The thermoelectric figure of merit at maximum ε_{\max}^i and the peak of maximum cooling rate, where FWHMs at maximum cooling rate peak are $\Gamma_r^p = \Gamma_x^p = 0.047$ eV and $\Gamma_y^p = 0.045$ eV. Data are obtained from Figs. 7-9.

FWHM	$\Gamma_i \rightarrow 0$			$\Gamma_i \rightarrow \Gamma_i^p$		
	$\varepsilon_{\max R}^i / \varepsilon_C$	$\varepsilon_{\max}^i / \varepsilon_C$	ZT	$\varepsilon_{\max R}^i / \varepsilon_C$	$\varepsilon_{\max}^i / \varepsilon_C$	ZT
k_r	0.1675	1	∞	0.0917	0.1314	1.0465
k_x	0.1579	0.8073	98.1559	0.0770	0.1046	0.8431
k_y	0.1445	0.7275	44.5247	0.0632	0.0825	0.6922

V. Conclusions

Thermoelectric heat engines and refrigerators are designed with 2D electronic reservoirs and momentum filters, including k_x -, k_y -, and k_r -filters. Differing from Ref. [23], the expressions of the performance parameters are derived by following the Fermi-Dirac distribution of electrons. After considering the resonant transport described by Lorentzian resonance, the parameters for heat engines and refrigerators are discussed and optimized. When the FWHM of Lorentzian resonance tends to be infinitesimal, the upper bounds of the parameters are found, such as maximum efficiency, EMP, maximum COP, COP at maximum χ , COP at maximum cooling rate and so on. Of which EMP and COP at maximum χ are the universal bounds with respect to the temperature ratio τ . Finally for more practical, the refrigerators with finite FWHM are chosen to discuss in detail. It is found that, for all three filtered cases, a value of FWHM can be chosen in

the range of $< 2k_B T$ for better thermoelectric performances if considering both the cooling rate and the thermoelectric figure of merit. Combining with all the discussions, one can find that k_r -filter seems the best for thermoelectric performances, then the k_x -filter, and then the k_y -filter. Therefore, these results may provide some guidance for designs of 2D thermoelectric devices, and the similar approaches can be applied to the 3D system under the Schrödinger picture. However, they cannot be adopted directly for the Dirac fermions which are also worth studying further.

Acknowledgements

X. Luo would like to thank Björn Sothmann for the meaningful discussion and advice. This work is supported by National Natural Science Foundation (No. 11365015), Program for New Century Excellent Talents in University of Ministry of Education of China (No. NCET-11-0096), and Research and Innovation Project for College Graduates of Jiangsu Province (No. CXZZ13_0081), People's Republic of China.

References

- [1] F. J. Disalvo, *Science* **285**, 703 (1999); L. E. Bell, *Science* **321**, 1457 (2008).
- [2] M. G. Kanatzidis, *Chem. Mater.* **22**, 648 (2010).
- [3] R. Venkatasubramanian, E. Siivola, T. Colpitts, and B. O'Quinn, *Nature* **413**, 597 (2001).
- [4] A. I. Hochbaum, R. Chen, R. D. Delgado, W. Liang, E. C. Garnett, M. Najarian, A. Majumdar, and P. Yang, *Nature* **451**, 163 (2008); A. I. Boukai, Y. Bunimovich, J. Tahir-Kheli, J. K. Yu, W. A. Goddard III, and J. R. Heath, *Nature* **451**, 168 (2008).
- [5] T. C. Harman, P. J. Taylor, M. P. Walsh, and B. E. LaForge, *Science* **297**, 2229 (2002).
- [6] G. J. Snyder and E. S. Toberer, *Nat. Mater.* **7**, 105 (2008); P. Pichanusakorn and P. Bandaru, *Mat. Sci. Eng. R* **67**, 19 (2010).
- [7] L. D. Hicks and M. S. Dresselhaus, *Phys. Rev. B* **47**, 12727 (1993); L. D. Hicks and M. S. Dresselhaus, *Phys. Rev. B* **47**, 16631 (1993).
- [8] G. D. Mahan and J. O. Sofo, *Proc. Natl. Acad. Sci. USA* **93**, 7436 (1996); M. S. Dresselhaus, G. Chen, M. Y. Tang, R. G. Yang, H. Lee, D. Z. Wang, Z. Ren, J. P. Fleurial, and P. Gogna, *Adv. Mater.* **19**, 1043 (2007); R. Kim, S. Datta, and M. S. Lundstrom, *J. Appl. Phys.* **105**, 034506 (2009).
- [9] A. Shakouri, *Annu. Rev. Mater. Res.* **41**, 399 (2011).
- [10] T. E. Humphrey, R. Newbury, R. P. Taylor, and H. Linke, *Phys. Rev. Lett.* **89**, 116801 (2002); T. E. Humphrey and H. Linke, *Phys. Rev. Lett.* **94**, 096601 (2005).
- [11] F. L. Curzon and B. Ahlborn, *Am. J. Phys.* **43**, 22 (1975).
- [12] C. de Tomás, A. C. Hernández, and J. M. M. Roco, *Phys. Rev. E* **85**, 010104(R) (2012).
- [13] Z. C. Tu, *J. Phys. A: Math. Theor.* **41**, 312003 (2008); R. Wang, J. Wang, J. He, and Y. Ma, *Phys. Rev. E* **87**, 042119 (2013).
- [14] M. Esposito, K. Lindenberg, and C. Van den Broeck, *EPL* **85**, 60010 (2009).
- [15] M. Esposito, R. Kawai, K. Lindenberg, and C. Van den Broeck, *Phys. Rev. Lett.* **105**, 150603 (2010).
- [16] H. Yan and H. Guo, *Phys. Rev. E* **85**, 011146 (2012); H. Yan and H. Guo, *Phys. Rev. E* **86**, 051135 (2012).
- [17] O. Karlström, H. Linke, G. Karlström, and A. Wacker, *Phys. Rev. B* **84**, 113415 (2011).
- [18] B. Muralidharan and M. Grifoni, *Phys. Rev. B* **85**, 155423 (2012).
- [19] B. Sothmann, R. Sánchez, A. N. Jordan, and M. Büttiker, *Phys. Rev. B* **85**, 205301 (2012); A. N. Jordan, B. Sothmann, R. Sánchez, and M. Büttiker, *Phys. Rev. B* **87**, 075312 (2013).
- [20] F. Chi, J. Zheng, Y. Liu, and Y. Guo, *Appl. Phys. Lett.* **100**, 233106 (2012).
- [21] R. S. Whitney, arXiv: 1306.0826.
- [22] D. Vashaee and A. Shakouri, *Phys. Rev. Lett.* **92**, 106103 (2004).
- [23] M. F. O'Dwyer, R. A. Lewis, C. Zhang, and T. E. Humphrey, *Phys. Rev. B* **72**, 205330 (2005).
- [24] L. Zhu, R. Ma, L. Sheng, M. Liu, and D. N. Sheng, *Phys. Rev. Lett.* **104**, 076804 (2010); Y. Ni, K. Yao, H. Fu, G. Gao, S. Zhu, and S. Wang, *Sci. Rep.* **3**, 1380 (2013); Y. Ni, K. Yao, H. Fu, G. Gao, S. Zhu, B. Luo, S. Wang, and R. Li, *Nanoscale* **5**, 4468 (2013).
- [25] Y. S. Hor, A. Richardella, P. Roushan, Y. Xia, J. G. Checkelsky, A. Yazdani, M. Z. Hasan, N. P. Ong, and R. J. Cava, *Phys. Rev. B* **79**, 195208 (2009).
- [26] W. Huang, H. Da, and G. Liang, *J. Appl. Phys.* **113**, 104304 (2013).

- [27] M. Rey, M. Strass, S. Kohler, P. Hänggi, and F. Sols, Phys. Rev. B **76**, 085337 (2007).
- [28] A. Levy and R. Kosloff, Phys. Rev. Lett. **108**, 070604 (2012).
- [29] Z. Bian and A. Shakouri, Appl. Phys. Lett. **88**, 012102 (2006); S. Wang and N. Mingo, Phys. Rev. B **79**, 115316 (2009).
- [30] S. Datta, *Electronic Transport in Mesoscopic Systems* (Cambridge University Press, Cambridge, England, 1995).
- [31] Z. Yan and J. Chen, J. Phys. D: Appl. Phys. **23**, 136 (1990).
- [32] Y. Wang, M. Li, Z. C. Tu, A. C. Hernández, and J. M. M. Roco, Phys. Rev. E **86**, 011127 (2012); Y. Izumida, K. Okuda, A. C. Hernández, and J. M. M. Roco, EPL **101**, 10005 (2013).
- [33] X. Luo, N. Liu, and J. He, Phys. Rev. E **87**, 022139 (2013).
- [34] J. Guo, J. Wang, Y. Wang, and J. Chen, Phys. Rev. E **87**, 012133 (2013).
- [35] Y. Apertet, H. Ouerdane, A. Michot, C. Goupil, and Ph. Lecoeur, EPL **103**, 40001 (2013).
- [36] X. Luo, C. Li, N. Liu, R. Li, J. He, and T. Qiu, Phys. Lett. A **377**, 1566 (2013).
- [37] N. Nakpathomkun, H. Q. Xu, and H. Linke, Phys. Rev. B **82**, 235428 (2010).
- [38] G. S. Nolas, J. Sharp, and H. J. Goldsmid, *Thermoelectrics: Basic Principles and New Materials Developments* (Springer, New York, 2001).